

Determination of leptoquark properties in polarized $e\gamma$ collisions

Michael A. Doncheski and Stephen Godfrey

Ottawa-Carleton Institute for Physics, Department of Physics, Carleton University, Ottawa, Canada K1S 5B6

(Received 18 July 1994)

We study leptoquark production using polarized $e\gamma$ colliders for the center-of-mass energies $\sqrt{s} = 500$ GeV and 1 TeV. We show that, using polarization asymmetries, the ten different types of leptoquarks listed by Buchmüller, Rückl, and Wyler can be distinguished from one another for leptoquark masses essentially up to the kinematic limit of the respective colliders. Thus, if a leptoquark were discovered, an $e\gamma$ collider could play a crucial role in determining its origins.

PACS number(s): 14.80.-j, 12.15.Ji, 13.88.+e, 14.70.Bh

There is much interest in the study of leptoquarks (LQ's), color (anti)triplet, spin 0 or 1 particles, which carry both baryon and lepton quantum numbers. Such objects appear in a large number of extensions of the standard model such as grand unified theories, technicolor, and composite models. Quite generally, the signature for leptoquarks is quite striking: a high p_T lepton balanced by a jet (or missing p_T balanced by a jet, for the νq decay mode, if applicable). Although the discovery of a leptoquark would be dramatic evidence for physics beyond the standard model it would lead to the question of which model the leptoquark originated from. Given the large number of leptoquark types it would be imperative to measure its properties to answer this question.

Following the notation of Buchmüller, Rückl, and Wyler (BRW) [1], the complete set of possible LQ's numbers 10 is S_1 , \tilde{S}_1 (scalar, isosinglet), R_2 , \tilde{R}_2 (scalar, isodoublet), S_3 (scalar, isotriplet), U_1 , \tilde{U}_1 (vector, isosinglet), V_2 , \tilde{V}_2 (vector, isodoublet), U_3 (vector, isotriplet). The production and corresponding decay signatures are quite similar, though not identical, and have been studied separately by many authors. Even focusing only on the Next Linear Collider (e^+e^- , $e\gamma$, and $\gamma\gamma$ modes), there is a considerable number of works in the literature [2-8]. The question arises as to how to differentiate between the different types. We propose to use a polarized $e\gamma$ collider to differentiate the LQ's: a polarized e beam [such as the SLAC Linear Collider (SLC)] in conjunction with a polarized laser backscattered photon beam. We concentrate on LQ production in $e\gamma$, which makes use of the fact that the hadronic component of the photon is important and cannot be neglected [5, 7, 9, 10]. An $e\gamma$ collider is the best choice for the production of LQ. Given a linear e^+e^- collider and backscattered laser technology, an e^+e^- , an $e\gamma$, and a $\gamma\gamma$ collider of roughly equal energy and luminosity are available at the same facility. The single LQ production rate at an e^+e^- collider will be lower than that at an $e\gamma$ collider since the quasi-real photon needed to supply the initial state quark is produced by radiation off one of the beams (i.e., a Weizsäcker-Williams photon), the effective energy and the luminosity in the e^+e^- case will be significantly lower than the $e\gamma$ case. Similarly, the initial e needed in the $\gamma\gamma$ case will be radiated by one of the γ beams (again, a Weizsäcker-Williams process),

again lowering the effective energy and the luminosity. Although the production of a LQ's in polarized $e\gamma$ collisions was considered first in Ref. [8], those authors do not use the polarization information to determine the specific model of a LQ.

We will assume that a peak in the e +jet invariant mass is observed in some collider (i.e., the existence of a LQ has been established), and so we need simply to identify the particular type of LQ. We assume that the leptoquark charge has not been determined and assume no intergenerational couplings. Furthermore, we will assume that only one of the ten possible types of LQ's is present. Table 2 of BRW gives information on the couplings to various quark and lepton combinations; the missing (and necessary) bit of information is that the quark and lepton have the same helicity (RR or LL) for scalar LQ production while they have opposite helicity (RL or LR) for vector LQ production. It is then possible to construct the cross sections for the various helicity combinations and consequently the double spin asymmetry, for the different types of LQ's. In the language of polarized collider phenomenology, the parton level asymmetry (denoted \hat{a}_{LL}) for any type of LQ is fully determined by the above information: $\hat{a}_{LL} = +1$ for a scalar LQ, and $\hat{a}_{LL} = -1$ for a vector LQ. The observable asymmetry (denoted A_{LL}) will, of course, differ from ± 1 due to the polarizability of the e and γ beams, and also due to the polarized parton distribution functions (which are related to the polarizability of the quarks within the polarized γ).

We will denote the various helicity cross sections as $\sigma^{\lambda_e \lambda_\gamma}$, $\lambda_i = +$ for R helicity, $\lambda_i = -$ for L helicity, and $\sigma_{\text{tot}} = \sigma^{++} + \sigma^{+-} + \sigma^{-+} + \sigma^{--}$. As is usual in the case of polarized collider phenomenology, it is useful to introduce the double longitudinal spin asymmetry A_{LL} ,

$$A_{LL} = \frac{(\sigma^{++} + \sigma^{--}) - (\sigma^{+-} + \sigma^{-+})}{(\sigma^{++} + \sigma^{--}) + (\sigma^{+-} + \sigma^{-+})} \quad (1)$$

and the helicity sum and difference distribution functions of partons within the photon:

$$f_{q/\gamma}(x, Q^2) = f_{q/\gamma}^+(x, Q^2) + f_{q/\gamma}^-(x, Q^2), \quad (2)$$

$$\Delta f_{q/\gamma}(x, Q^2) = f_{q/\gamma}^+(x, Q^2) - f_{q/\gamma}^-(x, Q^2),$$

where $f_{q/\gamma}^{+(-)}(x, Q^2)$ is the probability of a quark with the same (opposite) helicity as the photon to carry a fraction x of the photon's momentum. Unlike \hat{a}_{LL} , A_{LL} is an experimentally measurable quantity. It is then straightforward to construct A_{LL} for all ten types of LQ's in terms of

$\Delta f_{q/\gamma}(x, Q^2) = \Delta f_{\bar{q}/\gamma}(x, Q^2)$, $f_{q/\gamma}(x, Q^2) = f_{\bar{q}/\gamma}(x, Q^2)$, and $\kappa_{L,R}$ ($g_{L,R}^2/4\pi = \kappa_{L,R}\alpha_{em}$). There are three general cases.

(1) $\sigma^{+\lambda\gamma} = 0$ (only left-handed electrons couple to LQ):

$$A_{LL}(S_3) = \frac{\int_{M^2/s}^1 (dx/x) [\Delta f_{u/\gamma}(y, M^2) + 2\Delta f_{d/\gamma}(y, M^2)] f_{\gamma/e}(x)}{\int_{M^2/s}^1 (dx/x) [f_{u/\gamma}(y, M^2) + 2f_{d/\gamma}(y, M^2)] f_{\gamma/e}(x)}, \quad (3)$$

$$A_{LL}(\tilde{V}_2) = -\frac{\int_{M^2/s}^1 (dx/x) [\Delta f_{u/\gamma}(y, M^2)] f_{\gamma/e}(x)}{\int_{M^2/s}^1 (dx/x) [f_{u/\gamma}(y, M^2)] f_{\gamma/e}(x)}, \quad (4)$$

$$A_{LL}(U_3) = -\frac{\int_{M^2/s}^1 (dx/x) [\Delta f_{d/\gamma}(y, M^2) + 2\Delta f_{u/\gamma}(y, M^2)] f_{\gamma/e}(x)}{\int_{M^2/s}^1 (dx/x) [f_{d/\gamma}(y, M^2) + 2f_{u/\gamma}(y, M^2)] f_{\gamma/e}(x)}, \quad (5)$$

$$A_{LL}(\tilde{R}_2) = \frac{\int_{M^2/s}^1 (dx/x) [\Delta f_{d/\gamma}(y, M^2)] f_{\gamma/e}(x)}{\int_{M^2/s}^1 (dx/x) [f_{d/\gamma}(y, M^2)] f_{\gamma/e}(x)}. \quad (6)$$

(2) $\sigma^{-\lambda\gamma} = 0$ (only right-handed electrons couple to LQ):

$$A_{LL}(\tilde{S}_1) = \frac{\int_{M^2/s}^1 (dx/x) [\Delta f_{d/\gamma}(y, M^2)] f_{\gamma/e}(x)}{\int_{M^2/s}^1 (dx/x) [f_{d/\gamma}(y, M^2)] f_{\gamma/e}(x)}, \quad (7)$$

$$A_{LL}(\tilde{U}_1) = -\frac{\int_{M^2/s}^1 (dx/x) [\Delta f_{u/\gamma}(y, M^2)] f_{\gamma/e}(x)}{\int_{M^2/s}^1 (dx/x) [f_{u/\gamma}(y, M^2)] f_{\gamma/e}(x)}. \quad (8)$$

(3) $\sigma^{-\lambda\gamma}, \sigma^{+\lambda\gamma} \neq 0$ (both right- and left-handed electrons couple to LQ):

$$A_{LL}(S_1) = \frac{\int_{M^2/s}^1 (dx/x) [\Delta f_{u/\gamma}(y, M^2)] f_{\gamma/e}(x)}{\int_{M^2/s}^1 (dx/x) [f_{u/\gamma}(y, M^2)] f_{\gamma/e}(x)}, \quad (9)$$

$$A_{LL}(V_2) = -\frac{\int_{M^2/s}^1 (dx/x) \{ \kappa_R [\Delta f_{u/\gamma}(y, M^2) + \Delta f_{d/\gamma}(y, M^2)] + \kappa_L \Delta f_{d/\gamma}(y, M^2) \} f_{\gamma/e}(x)}{\int_{M^2/s}^1 (dx/x) \{ \kappa_R [f_{u/\gamma}(y, M^2) + f_{d/\gamma}(y, M^2)] + \kappa_L f_{d/\gamma}(y, M^2) \} f_{\gamma/e}(x)}, \quad (10)$$

$$A_{LL}(U_1) = -\frac{\int_{M^2/s}^1 (dx/x) [\Delta f_{d/\gamma}(y, M^2)] f_{\gamma/e}(x)}{\int_{M^2/s}^1 (dx/x) [f_{d/\gamma}(y, M^2)] f_{\gamma/e}(x)}, \quad (11)$$

$$A_{LL}(R_2) = \frac{\int_{M^2/s}^1 (dx/x) \{ \kappa_R [\Delta f_{u/\gamma}(y, M^2) + \Delta f_{d/\gamma}(y, M^2)] + \kappa_L \Delta f_{u/\gamma}(y, M^2) \} f_{\gamma/e}(x)}{\int_{M^2/s}^1 (dx/x) \{ \kappa_R [f_{u/\gamma}(y, M^2) + f_{d/\gamma}(y, M^2)] + \kappa_L f_{u/\gamma}(y, M^2) \} f_{\gamma/e}(x)}. \quad (12)$$

In all the above cases, the momentum fraction y of the quark within the photon is given by $y = M^2/(xs)$ and $f_{\gamma/e}(x)$ is the backscattered laser photon spectrum. The negative sign in front of the vector LQ asymmetries is a standard result; it comes about from the annihilation of two objects with opposite helicity into a vector particle. Another comment should be made at this time. Up to now, we have assumed that the beams will be polarized perfectly. This is probably not a bad assumption for the photon beam as the backscattered photon beam will carry the polarization of the incident laser beam, and it should be straightforward to polarize the laser to a very high degree. Electron beam polarizations of order 70% can be expected, and this will modify some of our argu-

ments. First, even if the LQ couples only to a particular helicity of electron, the contamination of the e beam with the wrong helicity will contaminate the signal. The finite polarization of the electron beam (λ_{beam}) will dilute the observable asymmetries by a factor λ_{beam} . Some care will have to be taken to ensure that any LQ signal observed with polarized beams is real, and is *not* due to contamination of the beam.

Having estimates of event numbers from previous works, we now need to determine if the different asymmetries predicted can be statistically separated. Because of a complete lack of data on parton distribution functions within a polarized photon, we need to use some theoretical input on the shapes of the helicity difference distribu-

tion functions of partons within the photon. There exist some parametrizations of the *asymptotic* polarized photon distribution functions [11, 12], where it is assumed that Q^2 and x are large enough that the vector meson dominance part of the photon structure is not important, but rather the behavior is dominated by the pointlike $\gamma q\bar{q}$ coupling. In this approximation, the distribution functions take the form

$$\Delta f_{q/\gamma}(x, Q^2) = \frac{\alpha}{\pi} \ln\left(\frac{Q^2}{\Lambda^2}\right) \frac{1}{x} \Delta p(x), \quad (13)$$

where $\Delta p(x)$ is a polynomial. In order to be consistent, we will use a similar asymptotic parametrization for the unpolarized photon distribution functions as well [13], even though various sets of more correct photon distribution functions exist (e.g., [14–17]). We will only use this asymptotic approximation in the unpolarized case only for the calculation of the asymmetry, where it is hoped that in taking a ratio of the asymptotic polarized to the asymptotic unpolarized photon distribution functions, the error introduced will be minimized; still, we suggest that our results be considered cautiously at

least in the relatively small LQ mass region. Our results should not be considered as hard predictions of the asymmetry A_{LL} , but rather a plausibility argument for this type of experimental analysis. We demonstrate the separability of the various LQ types, but a full analysis would make use of experimentally measured polarized and unpolarized parton distribution functions of the photon, when available. We note that in the asymptotic approximation, the unpolarized photon distribution functions have (not unexpectedly) a similar form to the polarized photon distribution functions:

$$f_{q/\gamma}(x, Q^2) = \frac{\alpha}{\pi} \ln\left(\frac{Q^2}{\Lambda^2}\right) \frac{1}{x^{1.6}} p(x), \quad (14)$$

where $p(x)$ is another polynomial. Finally, in regards to the question of the polarized photon distribution functions, a more careful calculation of the helicity difference distributions does exist [18] which includes the effect of VMD. However, the authors of Ref. [18] give parametrizations of the ratio of the helicity difference to the helicity sum distribution functions that are independent of Q^2 . These are reported to be valid for $10 \leq Q^2 \leq 100 \text{ GeV}^2$. Given the large mass of the LQ's being considered, the

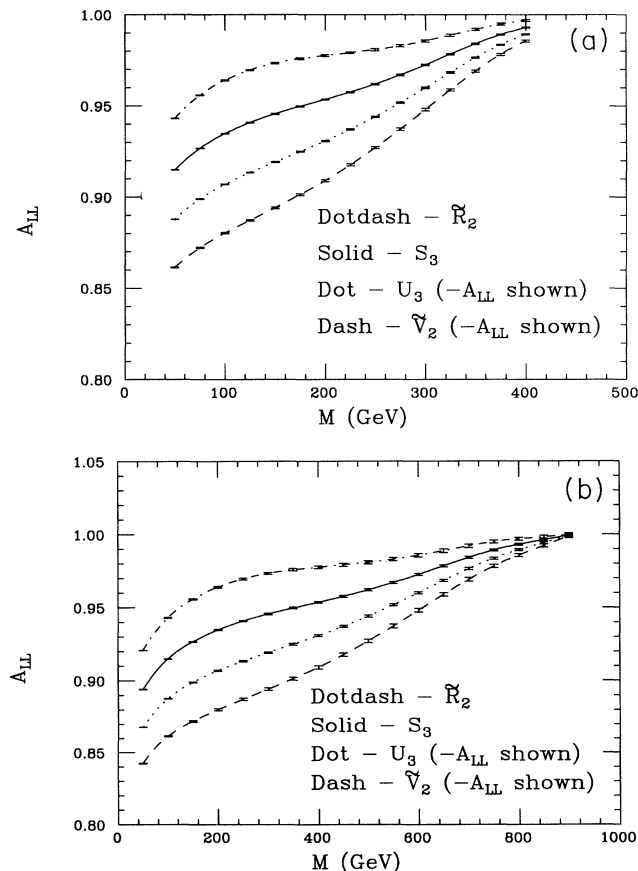


FIG. 1. A_{LL} vs M for LQ's which couple only to left-handed electrons; (a) is for a 500 GeV collider and (b) is for a 1 TeV collider. The solid curve is for an S_3 LQ, the dashed line is for a \tilde{V}_2 LQ ($-A_{LL}$ shown), the dotted line is for a U_3 LQ ($-A_{LL}$ shown), and the dot-dashed line is for a \tilde{R}_2 LQ.

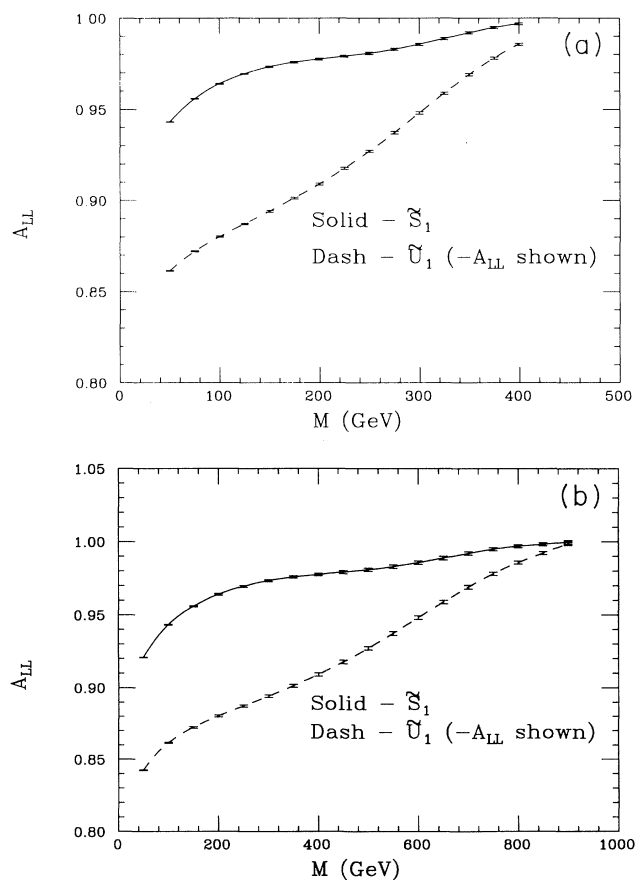


FIG. 2. A_{LL} vs M for LQ's which couple only to right-handed electrons; (a) is for a 500 GeV collider and (b) is for a 1 TeV collider. The solid curve is for an \tilde{S}_1 LQ and the dashed line is for a \tilde{U}_1 LQ ($-A_{LL}$ shown).

Q^2 is much too high to use these parametrizations.

We find that the asymmetry A_{LL} depends only on the dimensionless variable M/\sqrt{s} , though the event numbers depend on M and \sqrt{s} separately. For Figs. 1–5, (a) corresponds to the results at a 500 GeV e^+e^- collider operating in $e\gamma$ mode and (b) corresponds to a 1 TeV e^+e^- collider operating in $e\gamma$ mode. Throughout, we use an integrated luminosity of $50 \text{ fb}^{-1}/\text{yr}$ and the unpolarized photon distributions of Glück, Reya, and Vogt [16] to estimate the number of LQ events in a given LQ model. Also, unless noted otherwise, our results are for $\kappa_L = \kappa_R = 1$. The first step in determining the leptoquark couplings would be to use electron polarization to divide the leptoquarks into subsets that couple only to left-handed electrons, right-handed electrons, or to both. Once this is done the asymmetry can be used to distinguish between leptoquarks within these subsets. We show, in Fig. 1, A_{LL} vs M for the set of LQ's which couple only to left-handed electrons, that is, S_3 , U_3 , \tilde{V}_2 , and \tilde{R}_2 in the notation of BRW. The asymmetries for the vector LQ's (U_3 and \tilde{V}_2) have been multiplied by -1 in order to reduce the scale to the point that the structure in the

asymmetries is visible. That is, the scalar LQ's have positive values for A_{LL} while the vector LQ's have negative values for A_{LL} . In Fig. 2, we show A_{LL} vs M for the set of LQ's which couple only to right-handed electrons, that is \tilde{S}_1 and \tilde{U}_1 . We again multiply the vector LQ (\tilde{U}_1) asymmetry by -1 . Finally, in Figs. 3–5, we show A_{LL} vs M for the set of LQ's which couple to both helicities of electrons, that is S_1 , V_2 , U_1 , and R_2 . We again multiply the asymmetries of the vector LQ's (V_2 and U_1) by -1 . As the asymmetries for this set of LQ's depend on the arbitrary couplings κ_L and κ_R , we show results for various values of the κ s: in Fig. 3, $\kappa_L = \kappa_R = 1$, in Fig. 4, $\kappa_L = 1/2$ and $\kappa_R = 1$, and in Fig. 5, $\kappa_L = 1$ and $\kappa_R = 1/2$.

Using earlier results, (e.g., Fig. 3 of Ref. [7]), event numbers can be estimated and a statistical uncertainty in the measurement of A_{LL} (δA_{LL}) can also be estimated. For an asymmetry

$$A = \frac{\sigma(\alpha) - \sigma(\beta)}{\sigma(\alpha) + \sigma(\beta)}, \quad (15)$$

the statistical uncertainty δA_{LL} is given by the expres-

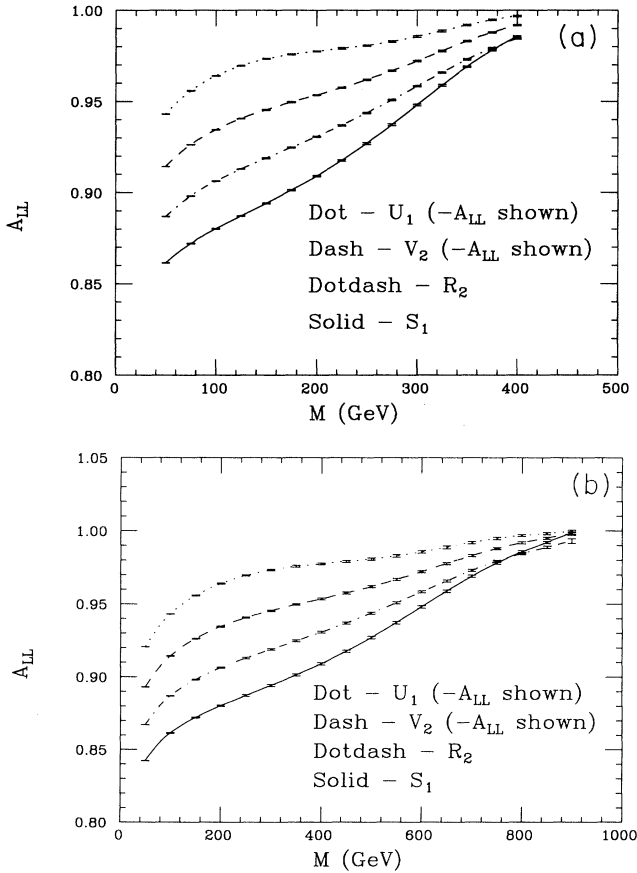


FIG. 3. A_{LL} vs M for LQ's which couple to both left- and right-handed electrons; (a) is for a 500 GeV collider and (b) is for a 1 TeV collider; here $\kappa_L = \kappa_R = 1$. The solid curve is for an S_1 LQ, the dashed line is for a V_2 LQ ($-A_{LL}$ shown), the dotted line is for a U_1 LQ ($-A_{LL}$ shown), and the dot-dashed line is for a R_2 LQ.

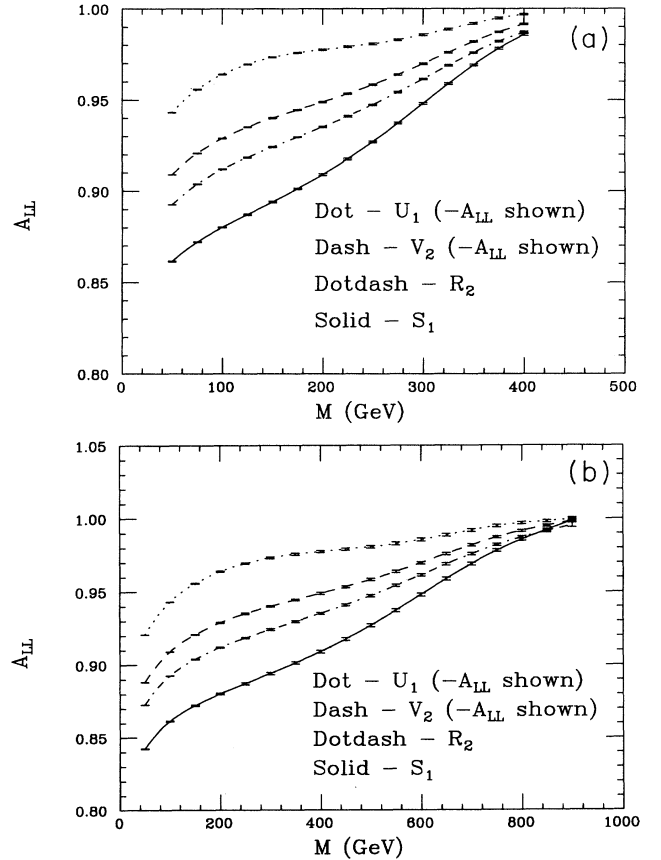


FIG. 4. A_{LL} vs M for LQ's which couple to both left- and right-handed electrons; (a) is for a 500 GeV collider and (b) is for a 1 TeV collider; here $\kappa_L = 0.5$ and $\kappa_R = 1$. The solid curve is for an S_1 LQ, the dashed line is for a V_2 LQ ($-A_{LL}$ shown), the dotted line is for a U_1 LQ ($-A_{LL}$ shown), and the dot-dashed line is for a R_2 LQ.

sion

$$\delta A_{LL} = \frac{1 - A^2}{\sqrt{1 - A}} \frac{1}{\sqrt{2N(\alpha)}} = \sqrt{\frac{1 - A^2}{N_{\text{tot}}}}, \quad (16)$$

where $N(\alpha)$ and N_{tot} are $L\sigma(\alpha)$ and $L[\sigma(\alpha) + \sigma(\beta)]$ respectively, with L being the integrated luminosity. These estimated δA_{LL} are shown in the error bars in Figs. 1–5. It can be seen that it is quite easy to distinguish a vector's LQ from a scalar LQ, as A_{LL} is large and positive for all the scalar LQ's while it is large and negative for vector LQ's. For a LQ which couples only to left-handed electrons (see Fig. 1), it will be possible to differentiate between the two possible vectors or scalar LQ's essentially up to the kinematical limit (remembering that the backscattered laser photon spectrum cuts off at an x of about 0.83; thus the maximum energy of an $e\gamma$ collider is slightly lower than the energy of the corresponding e^+e^- collider). If the LQ couples only to right-handed electrons (see Fig. 2), there is only one vector and one scalar LQ possible, so it will be possible to determine the particular LQ essentially up to the kinematical limit. Finally,

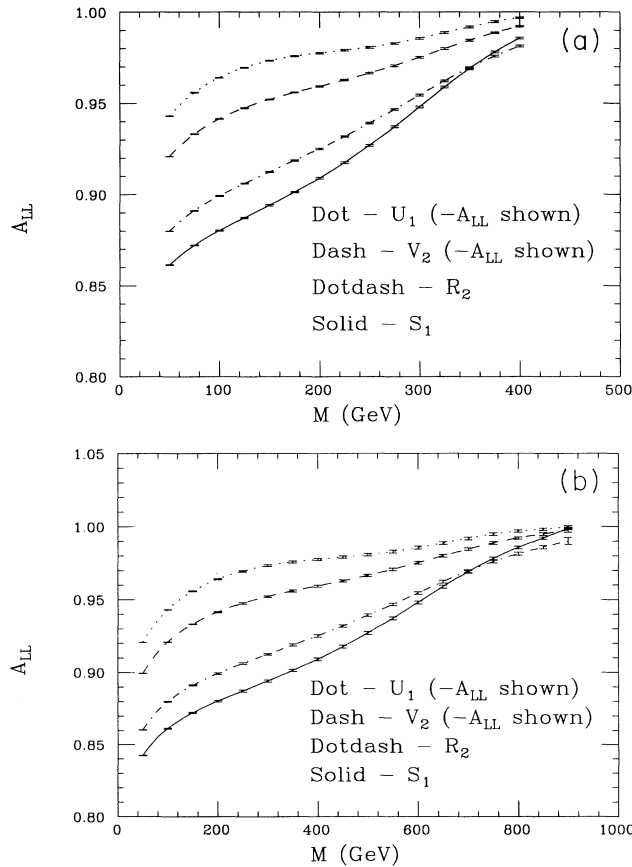


FIG. 5. A_{LL} vs M for LQ's which couple to both left- and right-handed electrons; (a) is for a 500 GeV collider and (b) is for a 1 TeV collider; here $\kappa_L = 1$ and $\kappa_R = 0.5$. The solid curve is for an S_1 LQ, the dashed line is for a V_2 LQ ($-A_{LL}$ shown), the dotted line is for a U_1 LQ ($-A_{LL}$ shown), and the dot-dashed line is for a R_2 LQ.

for a LQ which couples to both helicity electrons (see Figs. 3–5), it will be possible to differentiate between the two possible vectors or scalar LQ's essentially up to the kinematical limit, except for a small region of LQ mass where the asymmetries for the two types of scalar LQ are equal. The precise mass at which the crossover occurs depends on the values of $\kappa_{L,R}$. The limits quoted here assume a fully polarized electron beam; finite polarization will reduce these limits somewhat. A finite polarization of the e beam (λ_e) and the γ beam (λ_γ) will reduce the asymmetries given above by a factor $\lambda_e \lambda_\gamma$. This will also increase the statistical uncertainty, because of the dependence of δA_{LL} on A_{LL} itself, primarily in the large LQ mass region as A_{LL} will now differ considerably from 1. Assuming that $\lambda_e = 0.85$ and $\lambda_\gamma = 1$, we find that it is still possible to distinguish among the various different LQ's to a mass of about 350 GeV for a 500 GeV collider and about 700 GeV for a 1 TeV collider (the exact limits do depend on the particular LQ and the values of $\kappa_{L,R}$). In order to be a bit more quantitative, we compare, in Fig. 6, the asymmetries (with expected statistical uncertainties) the asymmetries for an \tilde{S}_1 and a \tilde{U}_1 LQ at a 500 GeV collider. This is a representative example of the full set of LQ types.

In conclusion, it certainly appears that a polarized $e\gamma$ collider can be used to differentiate between the different models of LQ's that can exist, essentially up to the kinematic limit of the $e\gamma$ collider. Furthermore, it is quite straightforward to distinguish scalar LQ's from vector LQ's for all LQ masses (given that the LQ is kinematically allowed) with only a polarized electron beam. It is thus clear that a more careful analysis is warranted, with the following improvements.

We rely on theoretical input for information on the parton distribution functions within a polarized photon; given the European Muon Collaboration (EMC) (proton) spin crisis, there may be some surprises in the polarized photon as well.

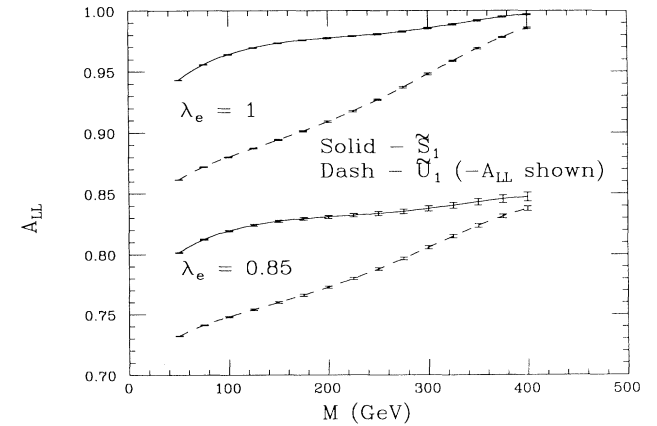


FIG. 6. A_{LL} vs M for LQ's which couple only to right-handed electrons at a 500 GeV collider. The solid curve is for an \tilde{S}_1 LQ and the dotted line is for a \tilde{U}_1 LQ ($-A_{LL}$ shown); the two sets of curves correspond to electron beam polarization $\lambda_e = 1$ and $\lambda_e = 0.85$ as labeled on the figure.

There are many questions as to the reliability of the asymptotic approximation to the photon distribution functions: Are the values of y (the momentum fraction of the quark within the photon) and Q^2 large enough that the photon behaves asymptotically? Is it possible, at the very least (in the absence of experimental data) to improve the theoretical input into the polarized photon distribution functions?

ACKNOWLEDGMENTS

This research was supported in part by the Natural Sciences and Engineering Research Council of Canada. The authors are grateful to Manuel Drees and Drew Peterson for helpful communications, to JoAnne Hewett for suggesting this particular analysis, and to Tom Rizzo for continual encouragement.

-
- [1] W. Buchmüller, R. Rückl, and D. Wyler, *Phys. Lett. B* **191**, 442 (1987).
- [2] H. Nadeau and D. London, *Phys. Rev. D* **47**, 3742 (1993).
- [3] J.L. Hewett and S. Pakvasa, *Phys. Lett. B* **227**, 178 (1989).
- [4] G. Bélanger, D. London, and H. Nadeau, *Phys. Rev. D* **49**, 3140 (1994).
- [5] J.E. Cieza Montalvo and O.J.P. Éboli, *Phys. Rev. D* **47**, 837 (1993).
- [6] O.J. Éboli, E.M. Gregores, M.B. Magro, P.G. Mercadante, and S.F. Novaes, *Phys. Lett. B* **311**, 147 (1993).
- [7] M.A. Doncheski and S. Godfrey, *Phys. Rev. D* **49**, 6220 (1994).
- [8] T.M. Aliev and Kh.A. Mustafaev, *Yad. Fiz.* **53**, 771 (1991) [*Sov. T. Nucl. Phys.* **53**, 482 (1991)].
- [9] M. Drees and R.M. Godbole, in *Proceedings of the Workshop on Physics and Experiments with Linear e^+e^- Colliders*, Waikoloa, Hawaii, 1993, edited by F. Harris *et al.* (World Scientific, Singapore, 1993), Vol. 2, p. 581; M. Drees, M. Krämer, J. Zunft, and P.M. Zerwas, *Phys. Lett. B* **306**, 371 (1993); O.J.P. Éboli, M.C. Gonzalez-Garcia, F. Halzen, and S.F. Novaes, *ibid.* **B 301**, 115 (1993); A.C. Bawa and W.J. Stirling, *Z. Phys. C* **57**, 165 (1993); M. Glück, E. Reya, and A. Weber, *Phys. Lett. B* **298**, 176 (1993); P. Chen, T.L. Barklow, and M.E. Peskin, *Phys. Rev. D* **49**, 3209 (1994); K.J. Abraham, *Phys. Lett. B* **316**, 365 (1993); E. Laenen, S. Riemersma, J. Smith, and W.L. van Neerven, *Phys. Rev. D* **49**, 5753 (1994).
- [10] CELLO Collaboration, H.-J. Behrend *et al.*, *Phys. Lett.* **126B**, 391 (1983); PLUTO Collaboration, Ch. Berger *et al.*, *ibid.* 111 (1984); Nucl. Phys. **B281**, 365 (1987); JADE Collaboration, W. Bartel *et al.*, *Z. Phys. C* **24**, 231 (1984); TASSO Collaboration, M. Althoff *et al.*, *ibid.* **C 31**, 527 (1986); TPC/Two-Gamma Collaboration, H. Aihara *et al.*, *Phys. Rev. Lett.* **58**, 97 (1987); *Z. Phys. C* **34**, 1 (1987); AMY Collaboration, T. Sasaki *et al.*, *Phys. Lett. B* **252**, 491 (1990); H1 Collaboration, I. Abt *et al.*, *ibid.* **314**, 436 (1993); OPAL Collaboration, R. Akers *et al.*, *Z. Phys. C* **61**, 357 (1994).
- [11] J.A. Hassan and D.J. Pilling, *Nucl. Phys.* **B187**, 563 (1981).
- [12] Z. Xu, *Phys. Rev. D* **30**, 1440 (1984).
- [13] A. Nicolaidis, *Nucl. Phys.* **B163**, 156 (1980).
- [14] D.W. Duke and J.F. Owens, *Phys. Rev. D* **26**, 1600 (1982).
- [15] M. Drees and K. Grassie, *Z. Phys. C* **28**, 451 (1985); M. Drees and R. Godbole, *Nucl. Phys.* **B339**, 355 (1990).
- [16] M. Glück, E. Reya, and A. Vogt, *Phys. Lett. B* **222**, 149 (1989); *Phys. Rev. D* **45**, 3986 (1992); **46**, 1973 (1992).
- [17] H. Abramowicz, K. Charchula, and A. Levy, *Phys. Lett. B* **269**, 458 (1991).
- [18] M. Glück and W. Vogelsang, *Z. Phys. C* **57**, 309 (1993).